Polarization directions of noncollinear phase-matched optical parametric downconversion output

A. Migdall

*Optical Technology Division, 221/B208, National Institute of Standards and Technology,
Gaithersburg, Maryland 20899*

An analysis of the output polarization of a noncollinear type I optical parametric downconversion source is presented. Such a source can be made by pumping a nonlinear crystal with an extraordinary-polarized beam to produce pairs of ordinary-polarized photons. A polarization map of the output light illustrates dramatic variation in the polarization direction at large scattering angles. The effect of this variation in polarization direction is seen on a map of the nonlinear conversion efficiency. The apparent ambiguity in the polarization for the particular case in which one of the outputs propagates along the crystal optic axis is also discussed. © 1997 Optical Society of America [S0740-3224(97)02005-5]

1. INTRODUCTION

Entangled two-particle photon states have proved to be a useful tool to investigate questions as fundamental as, "What is the nature of reality?" and "Is the quantum mechanical view an accurate representation of nature?"[1–5] While such questions often lead to confusion, or at least to a failure to comprehend the full ramifications of the theory, they are certainly useful in the attempt to comprehend the full nature of quantum mechanics. It is because the quantum mechanical representation of the physical world is so far from ordinary experience that misunderstandings are to be expected. The peculiar characteristics of quantum mechanics are especially highlighted in studies of inherently nonclassical entangled states. It is the counterintuitive nature of many of these studies that makes the field so important and exciting. See the paper by Pittman *et al.*[6] for one recent example of such a study.

Many of these fundamental studies rely particularly on the polarization of entangled photons. I point out an aspect of the polarization of typical two-photon sources used in these studies that I feel has not been generally appreciated. I present an analysis, mapping both the output polarization and the relative intensity of one type of entangled-photon source. This more comprehensive understanding of all the output polarization possibilities may allow for new, previously unconsidered tests of quantum mechanics.

Entangled-photon states are now most commonly produced by the process of optical parametric downconversion (PDC), in which photons from a pump beam, in effect, decay into pairs of photons (arbitrarily designated as signal and idler) within a nonlinear crystal medium.[7,8] This decay process occurs under the constraints of energy and momentum conservation (usually referred to as phase matching):

$$\omega_p = \omega_s + \omega_i, \tag{1a}$$

$$\mathbf{k}_p = \mathbf{k}_s + \mathbf{k}_i, \tag{1b}$$

where ω_p, ω_s, ω_i, $\mathbf{k}_p$, $\mathbf{k}_s$, and $\mathbf{k}_i$ are the respective frequencies and wave vectors of the pump, signal, and idler beams.

There are two ways, referred to as type I and type II phase matching, that these constraints may be met. In type I the downconverted photons propagate with the same polarization. That is, both photons are extraordinary rays (*e* rays), or both photons are ordinary rays (*o* rays), and the pump polarization is orthogonal to the downconverted photons. In type II, the downconverted photons propagate with opposite polarizations; that is, one photon is an *e* ray and the other photon is an *o* ray. In general, because these decay processes are nonresonant, the output light is spread over a wide range of wavelengths and over a wide range of angles relative to the incident pump direction. (Resonant cavities may be employed to enhance the production of downconverted light at particular wavelengths, but such configurations are not relevant to the discussion here.) The analysis described in this paper deals mainly with type I PDC from a negative uniaxial crystal with an *e*-ray pump going to two *o* rays, but has obvious extensions and applications to other crystals and to type II PDC.

Figure 1 shows the generic optical configuration of type I PDC. A correlated pair of signal and idler output photons of differing wavelengths are shown at angles A_s and A_i from the pump direction, which are all related through the phase-matching constraints of Eq. (1). This laboratory frame coordinate system is defined (without any loss of generality) so that the pump beam propagates along the x axis and the crystal optic axis $\mathbf{C}$ is in the x–z plane inclined at angle Θ with respect to the pump propagation direction. The phase-matching relationships also require
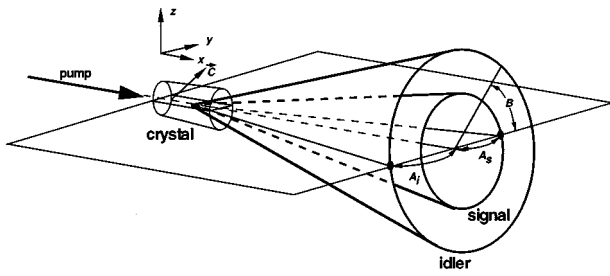
Fig. 1.   Pump beam, crystal, crystal optic axis **C**, and signal and idler PDC output cones at angles A_s and A_i.   The azimuthal coordinate angle B is referenced to the y-axis direction.

the pump and the signal and idler pair propagation directions to be constrained to a plane (i.e., $B_s = B_i + \pi$, where B_s and B_i are the azimuth angles of the signal and the idler output directions referenced to the y axis). Symmetry about the pump propagation direction allows pairs of photons to be emitted in a plane containing the pump direction and oriented along any azimuthal direction.   This results in output photons whose wavelengths vary with polar angle A, but are independent of azimuthal angle B.   [For describing the wavelength dependence of the PDC output, the $A-B$ coordinate system is most appropriate, although it is more convenient to start with the $\gamma-\phi$ system of Fig. 2 (described next) to deal with the polarization of the output.]

2.   ANALYSIS OF PDC POLARIZATION

To understand the output polarization directions of the PDC process, it is useful to consider the definitions of o and e rays.   For a light ray propagating along an arbitrary direction within a uniaxial crystal, the polarization directions of o and e rays are determined by the crystal optic axis and the ray propagation directions.[9]   An e ray is polarized in the plane containing the propagation direction and the crystal optic axis.   The polarization direction of an o ray is oriented perpendicular to the optic axis and perpendicular to the direction of propagation.

These definitions of o and e rays are used to determine the polarization of the output of type I PDC.   The analysis presented here is for the particular PDC configuration in which an e-ray pump produces two o-ray output photons ($e \rightarrow o, o$).   For a pump propagation along the x axis, this defines the pump polarization to be along the z axis as shown in Fig. 2.   (The following analysis could just as well handle the less common $o \rightarrow e, e$ type I PDC configuration.)   The initial questions asked about the PDC output are, "What is the polarization of the output at a given angle (A) from the pump direction?" and "How does it vary as a function of azimuthal angle (B)?"   These are answered with the definition of an o ray propagating along the (A, B) direction:

$$\mathbf{P}(A, B) \cdot \mathbf{C}(\Theta) = 0, \tag{2}$$

where $\mathbf{P}(A, B)$ is the polarization direction of downconverted output light propagating along the direction (A, B) and $\mathbf{C}(\Theta)$ is the optic-axis direction.   In lab situations it is useful to define the polarization angle of an output photon propagating along the (A, B) direction as

the angle β referenced to the z'' axis as shown in Fig. 2. This angle is the rotation from the z'' axis in the $x''-z''$ plane.   The transformations between the $x-y-z$, $x'-y'-z'$, and $x''-y''-z''$ frames are defined by a rotation of angle ϕ about the z axis to get to the $x'-y'-z'$ frame. (Note that $z = z'$.)   A rotation of angle γ about the y' axis completes the transformation to the $x''-y''-z''$ frame.

P and **C** are written in terms of γ, ϕ, β, and Θ (γ and ϕ are latitude and longitude coordinates as defined in Fig. 2) and inserted into Eq. (2), yielding the output-polarization angle:

$$\beta = \tan^{-1}\left[\frac{-\cos\Theta\,\cos\phi\,\sin\gamma + \sin\Theta\,\cos\gamma}{\cos\Theta\,\sin\phi}\right]. \tag{3}$$

Transforming from (ϕ, γ) coordinates to (A, B) coordinates, using the relations

$$\phi = \tan^{-1}[\tan A\,\cos B],$$

$$\gamma = \sin^{-1}[\sin A\,\sin B], \tag{4}$$

allows the polarization to be plotted versus the azimuthal angle, as is shown in Fig. 3(a) for the case in which the optic axis is tilted at 35.3° from the x axis.   (This particular angle was chosen to meet the needs of a PDC photon pair experiment to measure absolute IR radiance using only a visible detector, similar to an experiment proposed by Klyshko.[10])   Here the results are presented in terms of the $A-B$ coordinate system to show how the polarization varies with azimuthal angle B for a given wavelength, since the wavelength of the PDC output is a function of angle A only.

For small polar output angles (PDC output direction close to the pump direction) we get the familiar result: The polarization of the output is horizontal, i.e., perpendicular to the pump polarization.   As A increases, though, β starts to deviate from 90°; only at $B = 90$° and $B = 270$° does β equal the accustomed result.   As A becomes larger than Θ, β starts to wrap around past π.   To explain this behavior, it is useful to plot a (ϕ, γ) map of β as shown in Fig. 3(b).   The angles of the dashes at each point (ϕ, γ) indicate the polarization direction of downconverted light emitted along that (ϕ, γ) direction.   This map shows how the polarization varies with its emission direc-
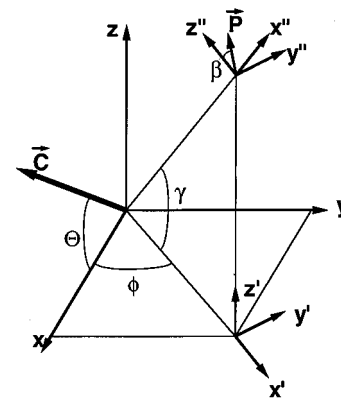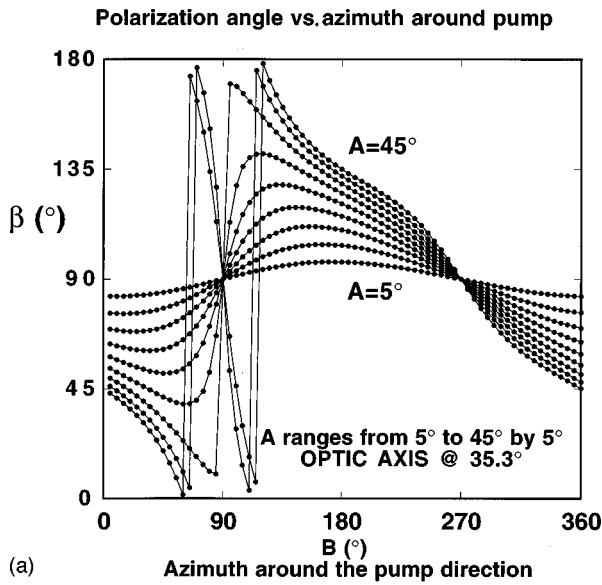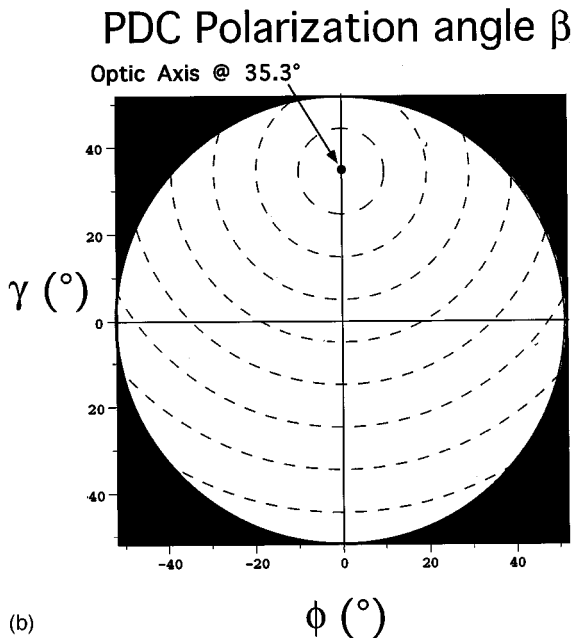

Fig. 2. ϕ, γ, β, coordinate system and the crystal optic axis tilted by angle Θ in the $x-z$ plane; β is the angle between z'' and **P** in the $x''-z''$ plane.

Polarization angle vs. azimuth around pump

(a)

PDC Polarization angle β

Optic Axis @ 35.3°

(b)

Fig. 3. (a) Polarization angle β versus azimuthal angle B for various polar output angles A. (For polarization, 0° and 180° are not physically distinct, so the discontinuities shown are indicative of a nonzero winding number of the polarization direction.) (b) Polarization of PDC light emitted along any direction (ϕ, γ) is indicated by the *angle* of the dashes at that location. The center of symmetry at $(\phi, \gamma) = (0°, 35.3°)$ coincides with the crystal optic axis tilt, indicated by the black dot.

tion (ϕ, γ). From this view, it becomes clear that the output polarization directions are simply described by circles centered around the optic axis (tilted at $\phi = 0°$, $\gamma = 35.3°$). This shows only that an o-ray polarization must be perpendicular to the optic axis. [This is an example of the importance of choosing the appropriate coordinate system to best explain particular aspects of this problem. Figure 3(b) shows that the rather complicated looking Eq. (3) is just the formula, in polar coordinates, for a family of concentric circles with a center offset from the coordinate system origin.]

From Fig. 3(b) it is also seen that PDC light emitted in the vicinity of the optic axis is clearly a special case. The polarization may have any orientation, depending on how the emission direction deviates from the optic axis, whereas the polarization of light emitted precisely along the optic axis does not appear to be well defined. This is because, for light emitted along the optic axis, any polarization direction will be orthogonal to the optic axis and thus will be an o-ray. To further explain this peculiar region, the PDC conversion efficiency must be investigated.

3. EFFECT OF POLARIZATION ON PDC CONVERSION EFFICIENCY

Besides the polarization of the output, the PDC conversion efficiency was also mapped. This problem was solved by calculating the equivalent, but more convenient, reverse problem, in which the signal and idler beams (both o rays) are input into the crystal at appropriate angles to produce a sum-frequency e-ray beam at the pump frequency and to propagate along the pump-laser direction. (The analysis here assumes a short crystal interaction length, so that beam walk-off effects can be neglected. For a good description of walk-off effects see the work of Koch et $al.$[11]) For a particular signal wavelength, the phase-matching and energy-conservation conditions were used to determine the idler energy and the polar input angles for the signal and idler light. From these angles and the choice of an azimuthal angle, which determine the signal and idler polarization directions through Eq. (3), the x, y, and z components of the signal and idler electric fields were obtained. These, along with the contracted nonlinear coefficient matrix D for the nonlinear crystal,[12] give the polarization at the pump or sum-frequency beam as follows:

$$\mathbf{P}(\omega_s + \omega_i) = D \begin{pmatrix} E_x(\omega_s)E_x(\omega_i) \\ E_y(\omega_s)E_y(\omega_i) \\ E_z(\omega_s)E_z(\omega_i) \\ E_y(\omega_s)E_z(\omega_i) + E_z(\omega_s)E_y(\omega_i) \\ E_z(\omega_s)E_x(\omega_i) + E_x(\omega_s)E_z(\omega_i) \\ E_x(\omega_s)E_y(\omega_i) + E_y(\omega_s)E_x(\omega_i) \end{pmatrix} .$$

(5)

Because the pump wave must be an e ray to propagate in a phase-matched manner, only the z component of $\mathbf{P}$ is important.

This particular calculation was done for a LiIO$_3$ crystal with its optic axis tilted in the x–z plane at 35.3° (as in Section 2) from the x axis, with a pump beam at 457.9 nm propagating along the x axis. The D matrix for LiIO$_3$, which has class 6 symmetry,[12] with Kleinman symmetry assumed,[13] is

$$D = \begin{bmatrix} 0 & 0 & 0 & 0 & d_{31} & 0 \\ 0 & 0 & 0 & d_{31} & 0 & 0 \\ d_{31} & d_{31} & d_{33} & 0 & 0 & 0 \end{bmatrix},$$

(6)

where the ratio d_{33}/d_{31} is taken to be 1 for LiIO$_3$, as recommended by Choy and Byer.[14] Since we are interested in only relative results, d_{31} was defined as 1. The refractive indices used for the LiIO$_3$ phase matching were those also listed in Choy and Byer. Because the D matrix given in Eq. (6) was defined for a coordinate system with

the z axis along the crystal optic axis **C**, the electric fields were transformed into the crystal frame before multiplication by D, and **P** was then transformed back into the laboratory frame ($x-y-z$ of Fig. 2).

Figure 4 is a relative map of the square of the z component of the polarization produced at the pump frequency by the action of the signal and idler beams, which are input at the appropriate phase-matched angles ϕ and γ and calculated with Eq. (5). This is equivalent to the conversion efficiency of the spontaneous process of downconversion from the pump beam into signal and idler beams. The large annulus in the right-hand panel of Fig. 4 covers the idler spectral range from 2.5 μm at the inner edge to 9.0 μm at the outer edge. The complementary signal spectral range, from 0.478 μm at the inner edge to 0.56 μm at the outer edge, is shown as the expanded annulus in the left-hand panel. (It is useful to note that correlated signal and idler points in the two annuli must have identical efficiencies, so one annulus maps onto the other in an inside-out, upside-down fashion.)

The most notable features of the efficiency map are the two regions on either side of the optic axis, where the conversion efficiency becomes very small. These regions coincide with the regions where the polarization of the IR downconverted light is vertical, while the regions of IR horizontal polarization yield the highest efficiencies.

Note that the visible signal photons are all roughly horizontally polarized, regardless of the polarization of their IR twins.

Alternately, one can calculate the effective scalar quantity d_{eff}, as defined by the relation $P(\omega_s + \omega_i) = d_{\text{eff}} E(\omega_s) E(\omega_i)$. For this calculation it is best to stay in the crystal frame coordinate system defined as $z_c = \mathbf{C}$, $y_c = y$, and x_c rotated by $\pi/2 - \Theta$ from the x axis. Because the signal and idler beams are o rays, their electric fields may be written generally as $\mathbf{E}_s = E_s(\hat{x}_c \sin v + \hat{y}_c \cos v)$ and $\mathbf{E}_i = E_i(\hat{x}_c \sin w + \hat{y}_c \cos w)$, where $E_{s,i}$ are the amplitudes and v and w define the signal and the idler polarizations, respectively, in the crystal coordinate frame. Inserting these fields into Eq. (5), with D given by Eq. (6), results in many zero terms, leaving only one nonzero component of **P**:

$$P_{z_c}(\omega_s + \omega_i) = d_{31}[E_{x_c}(\omega_s)E_{x_c}(\omega_i) + E_{y_c}(\omega_s)E_{y_c}(\omega_i)]$$

$$= d_{31}(\sin v \, \sin w + \cos v \, \cos w)E_s E_i$$

$$= d_{31} \cos(v - w)E_s E_i. \tag{7}$$

Transforming this back into the $x-y-z$ lab frame gives

$$P_z(\omega_s + \omega_i) = d_{31} \sin \Theta \, \cos(v - w)E_s E_i, \tag{8}$$
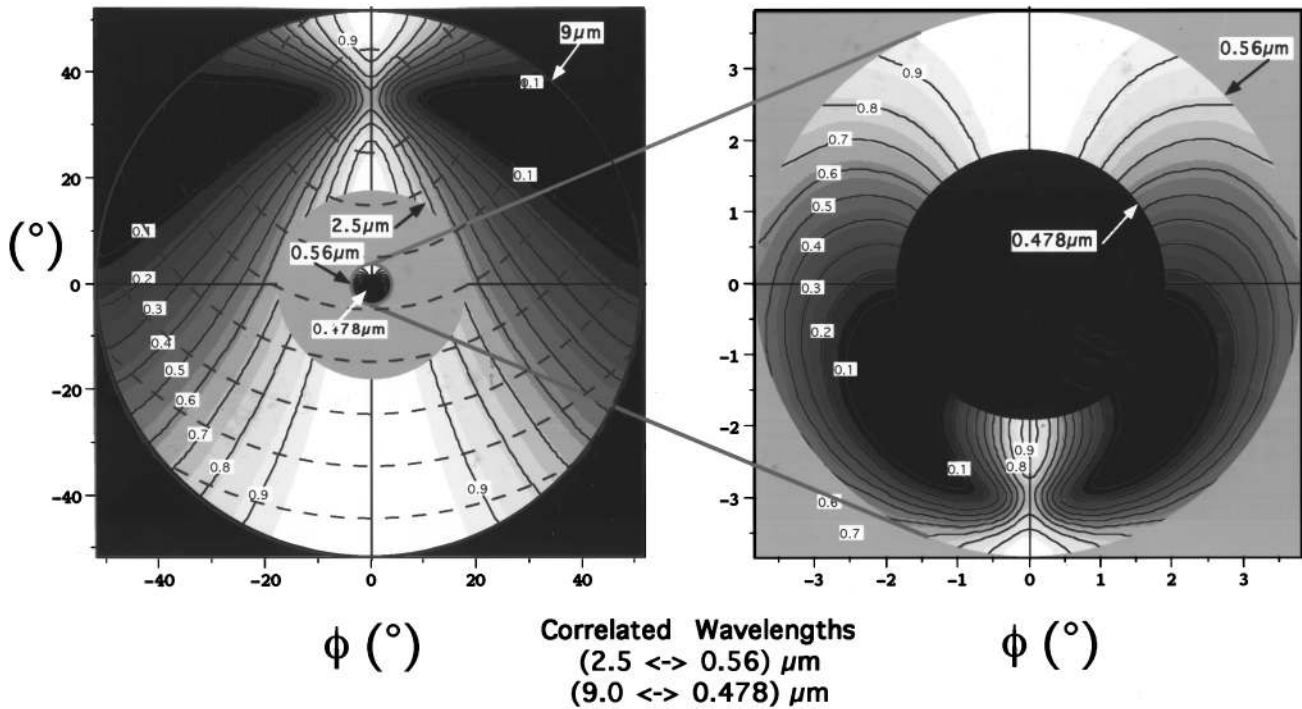
so d_{eff} is then just

Fig. 4. Left, relative map of PDC conversion efficiency versus ϕ and γ. To guide the eye, the gray scale from white to black indicates the graduation from high to low efficiency. The outer annulus covers the directions of idler output in the spectral region from 2.5 μm to 9.0 μm. The overlaid dashes show the polarization directions of PDC output light. (The efficiency along the positive γ axis near the optic axis is unity. The fact that the contours cut across the axis is an artifact of the contour plotting routine.) Right, the inner annulus covering the signal output directions is shown enlarged. The spectral range of this annulus covers 0.478 μm at its inner edge to 0.560 μm at the outer edge. This region is correlated to the 2.5–9.0 μm idler spectral range of the outer annulus.

$$d_{\mathrm{eff}} = d_{31} \cos \Theta \cos(v - w). \qquad (9)$$

From this form it becomes clear that the efficiency for this PDC configuration depends on the difference between the signal and the idler polarization angles, rather than on each individual angle. The d_{eff} reaches a maximum for parallel signal and idler polarizations and a minimum for perpendicular polarizations. Also, as a test, Eq. (9) reduces to $d_{\mathrm{eff}} = d_{13} \sin \Theta$ for the collinear case (where $A_s = A_i = 0$), which agrees with the result for this crystal class and configuration given by Zernike and Midwinter.[12]

4. DISCUSSION OF RESULTS

The region of parameter space in which most PDC work has been done is with both the signal and the idler output beams nearly collinear with the pump beam, even in the noncollinear experiments. This region is near the origin of Figs. 3(b) and 4 (ϕ and $\gamma \ll \Theta$). It is only when the output angles become significant compared with the crystal optic axis tilt that the polarization variation becomes noticeable. For instance, when $A = \Theta$, the polarization angle reaches 45° at $B = 0°$. One such experiment, which is currently underway and that operates in this regime, uses PDC to measure absolute radiance on the IR. This application, based on the concept proposed by Klyshko,[10] uses IR–visible photon pairs far from the equal-angle, degenerate case.

While entangled-photon tests of quantum mechanics have so far operated in the small-angle region, this clearer picture of the output PDC polarization may open new possibilities. From Fig. 4 it is clear that type I PDC can produce photon pairs with parallel polarizations (both photons emitted in the $\phi = 0$ plane), pairs with nearly perpendicular polarizations (albeit with reduced efficiency), or any value in between. So it is not necessary to use a wave plate to rotate the polarization of one photon of a pair or to go to type II PDC to produce orthogonally polarized pairs of photons.

It is worth noting two configurations that may be used to different advantages, depending on the particular application. If a detector is scanned in the horizontal plane at $\gamma = 0$ with the crystal optic axis tilted in the vertical direction, one will see variation of the PDC polarization (see Fig. 4). If this is not desired, the polarization variation can be eliminated by tilting the optic axis in the horizontal plane so that no change in polarization will be seen as a detector is scanned horizontally.

One final interesting region occurs when one looks at the polarization of the downconverted photons emitted along the optic axis. In that case, for type I PDC, all polarization directions will be o rays, because all will be perpendicular to the optic axis. From Fig. 4 this appears to allow for the production of a pair of correlated photons, where one photon polarization is well defined and the other photon polarization can have any value. A look at the conversion efficiency map shows that, in the regions where the downconverted output polarization approaches vertical, the coupling to the pump beam falls off. This means that a measurement of the polarization of the type I PDC output would show the intensity disappearing as the polarization nears vertical. At any infinitesimal point near the optic axis, the output polarization would be well defined, but finite resolution (from finite aperture size, diffraction limits, phase-match uncertainty, or similar effects) in this region would require an average over a range of polarizations. For regions close enough to the optic axis to allow a range of polarizations to be viewed indistinguishably, the PDC output would have to be averaged to determine what polarization would be observed. It is also interesting that, although the output near this region would have a high polarization variation, the polarization of the twin photon would be nearly constant. This unique situation may prove useful for future entangled-state tests.

Other phase-matching configurations can have similarly interesting results. The other type I arrangement, where an o-ray pump beam produces two e-ray outputs, also yields an effect for output propagating along the optic axis. A polarization map for this case would show all output polarization directions oriented along radii centered on the optic axis. Since a beam propagating along the optic axis cannot be an e ray, one might expect the conversion efficiency to drop to zero near this region. It is interesting that in the $o \rightarrow e$, e phase-matching case the polarization definitions allow no output along the optic axis, whereas in the previously considered $e \rightarrow o$, o case any polarization orientation is allowed. Type II phase-matching should also exhibit similar suppression of PDC output for e-ray emission along the optic axis, whereas o-ray emission can vary widely in the vicinity of the optic axis. Although from this discussion the output polarization of other PDC phase-match configurations can be qualitatively understood, they certainly warrant further study.

5. CONCLUSION

I have presented a complete map of the output polarization of type I $e \rightarrow o$, o PDC (which may be straightforwardly extended to type I $o \rightarrow e$, e and to type II). This makes it clear that type I PDC cannot be said simply to produce output with polarization perpendicular to the pump polarization. The analysis has highlighted a range of new polarization configurations that have not generally been recognized. This awareness may stimulate new applications of entangled-photon states, allowing further interesting tests of fundamental physical questions.

REFERENCES AND NOTES

1. A. Einstein, B. Podolsky, and N. Rosen, "Can quantum-mechanical description of physical reality be considered complete?" Phys. Rev. **47**, 777–780 (1935).
2. Z. Y. Ou and L. Mandel, "Violation of Bell's inequality and classical probability in a two-photon correlation experiment," Phys. Rev. Lett. **61**, 50–53 (1988).
3. Y. H. Shih and C. O. Alley, "New type of Einstein–

A. Migdall

Podolsky–Rosen–Bohm experiment using pairs of light quanta produced by optical parametric downconversion," Phys. Rev. Lett. **61**, 2921–2924 (1988).

4. T. E. Kiess, Y. H. Shih, A. V. Sergienko, and C. O. Alley, "Einstein–Podolsky–Rosen–Bohm experiment using pairs of light quanta produced by type-II parametric downconversion," Phys. Rev. Lett. **71**, 3893–3897 (1993).

5. R. Y. Chiao, P. G. Kwait, and A. Steinberg, "Quantum nonlocality in two-photon experiments at Berkeley," Quantum Semiclassic. Opt. **7**, 259–278 (1995).

6. T. B. Pittman, D. V. Strekalov, A. Migdall, M. H. Rubin, A. V. Sergienko, and Y. H. Shih, "Can two-photon interference be considered the interference of two-photon?" Phys. Rev. Lett. **77**, 1917–1920 (1996).

7. A. Yariv, *Optical Electronics*, 3rd ed. (Holt, Rinehart, & Winston, New York, 1985), Chap. 8, pp. 227–273.

8. D. N. Klyshko, *Photons and Nonlinear Optics* (Gordon & Breach, New York, 1988), Chap. 1, pp. 1–64; Chap. 6, pp. 285–357.

9. M. Born and E. Wolf, *Principles of Optics*, 6th ed. (Pergamon, New York, 1993), pp. 679–680.

10. D. N. Klyshko, "Utilization of vacuum fluctuations as an optical brightness standard," Sov. J. Quantum Electron. **7**, 591–595 (1977).

11. K. Koch, E. C. Cheung, G. T. Moore, S. H. Chakmakjian, and J. M. Liu, "Hot spots in parametric fluorescence with pump beam of finite cross section," IEEE J. Quantum Electron. **31**, 769–781 (1995).

12. F. Zernike and J. E. Midwinter, *Applied Nonlinear Optics* (Wiley, New York, 1973), pp. 34–41.

13. Although this Kleinman symmetry assumption is best met for wavelengths shorter than 5 μm, where $LiIO_3$ transmittance begins to fall off, the calculations here are carried out to 9 μm for better viewing of the results.

14. M. Choy and R. L. Byer, "Accurate second-order susceptibility measurements of visible and infrared nonlinear crystals," Phys. Rev. B **14**, 1693–1706 (1976).